

Constraints on the Reheating Temperature in Gravitino Dark Matter Scenarios

Josef Pradler^{1,*} and Frank Daniel Steffen^{1,†}

¹*Max-Planck-Institut für Physik, Föhringer Ring 6, D-80805 Munich, Germany*

Considering gravitino dark matter scenarios, we study constraints on the reheating temperature of inflation. We present the gauge-invariant result for the thermally produced gravitino yield to leading order in the Standard Model gauge couplings. Within the framework of the constrained minimal supersymmetric Standard Model (CMSSM), we find a maximum reheating temperature of about 10^7 GeV taking into account bound-state effects on the primordial ${}^6\text{Li}$ abundance. We show that late-time entropy production can relax this constraint significantly. Only with a substantial entropy release after the decoupling of the lightest Standard Model superpartner, thermal leptogenesis remains a viable explanation of the cosmic baryon asymmetry within the CMSSM.

PACS numbers: 98.80.Cq, 95.35.+d, 12.60.Jv, 95.30.Cq

INTRODUCTION

The observed flatness, isotropy, and homogeneity of the Universe suggest that its earliest moments were governed by inflation [1, 2]. The inflationary expansion is followed by a phase in which the Universe is reheated. The reheating process repopulates the Universe and provides the initial conditions for the subsequent radiation-dominated epoch. We refer to the reheating temperature T_R as the initial temperature of this early radiation-dominated epoch of our Universe.

The value of T_R is an important prediction of inflation models. While we do not have evidence for temperatures of the Universe higher than $\mathcal{O}(1 \text{ MeV})$ (i.e., the temperature required by primordial nucleosynthesis), inflation models can point to T_R well above 10^{10} GeV [2, 3].

In this Letter we consider supersymmetric (SUSY) extensions of the Standard Model in which the gravitino \tilde{G} is the lightest supersymmetric particle (LSP) and stable because of R-parity conservation. The gravitino LSP is a well-motivated dark matter candidate. As the gauge field of local SUSY transformations and the spin-3/2 superpartner of the graviton, the gravitino is an unavoidable implication of SUSY theories including gravity [4]. Its interactions are suppressed by inverse powers of the (reduced) Planck scale $M_P = 2.4 \times 10^{18}$ GeV. Its mass $m_{\tilde{G}}$ results from spontaneous SUSY breaking and can range from the eV scale up to scales beyond the TeV region [5].

While any initial population of gravitinos must be diluted away by the exponential expansion during inflation [6], gravitinos are regenerated in scattering processes of particles that are in thermal equilibrium with the hot primordial plasma. The efficiency of this thermal production of gravitinos during the radiation-dominated epoch is sensitive to T_R [7, 8, 9, 10, 11]. Since the resulting gravitino density $\Omega_{\tilde{G}}^{\text{TP}}$ is bounded from above by the dark matter density Ω_{dm} , upper bounds on T_R can be derived [8, 12, 13, 14, 15]. These bounds can be compared with predictions of the reheating temperature T_R from inflation models. Moreover, T_R is important for our

understanding of the cosmic baryon asymmetry. For example, successful standard thermal leptogenesis [16] requires $T_R \gtrsim 10^9$ GeV [17].

We update the T_R limits using the full gauge-invariant result for the relic density of thermally produced gravitinos, $\Omega_{\tilde{G}}^{\text{TP}}$, to leading order in the Standard Model gauge couplings [11]. This allows us to illustrate the dependence of the bounds on the gaugino-mass relation at the scale of grand unification $M_{\text{GUT}} \simeq 2 \times 10^{16}$ GeV.

We consider gravitino dark matter scenarios also in the framework of the constrained minimal supersymmetric Standard Model (CMSSM) in which the gaugino masses, the scalar masses, and the trilinear scalar interactions are assumed to take on the respective universal values $m_{1/2}$, m_0 , and A_0 at M_{GUT} . Taking into account gravitinos from thermal production and from late decays of the lightest Standard Model superpartner, we provide new upper bounds on the reheating temperature in the $(m_{1/2}, m_0)$ plane for various values of $m_{\tilde{G}}$. Previous studies of T_R constraints within the CMSSM used the result of [10] to explore the viability of $T_R \gtrsim 10^9$ GeV [13, 14]. Our study presents also scans for T_R as low as 10^7 GeV based on the result of [11] which includes electroweak contributions to thermal gravitino production [18].

In the considered CMSSM scenarios with the gravitino LSP, the next-to-lightest SUSY particle (NLSP) is either the lightest neutralino $\tilde{\chi}_1^0$ or the lighter stau $\tilde{\tau}_1$.¹ Because of the extremely weak interactions of the gravitino, the NLSP typically has a long lifetime before it decays into the gravitino. If these decays occur during or after big-bang nucleosynthesis (BBN), the Standard Model particles emitted in addition to the gravitino can affect the abundance of the primordial light elements. Indeed, these BBN constraints disfavor the $\tilde{\chi}_1^0$ NLSP for $m_{\tilde{G}} \gtrsim 100$ MeV [13, 14, 21]. For the slepton NLSP case, the BBN constraints associated with

¹ For simplicity, we consider $A_0 = 0$ in this work. For sizable $|A_0|$, also the lighter stop \tilde{t}_1 can be the NLSP [19, 20].

hadronic/electromagnetic energy injection have also been estimated and found to be much weaker but still significant in much of the parameter space [13, 14, 15, 21].

Only recently, it has been stressed that bound-state formation of long-lived negatively charged particles with the primordial nuclei can affect BBN [22, 23, 24, 25]. With the charged long-lived stau NLSP, these bound-state effects also apply to the considered gravitino dark matter scenarios. In particular, a significant enhancement of ${}^6\text{Li}$ production has been found to imply severe upper limits on the $\tilde{\tau}_1$ NLSP abundance prior to decay [22] which strongly restricts the mass spectrum in the $\tilde{\tau}_1$ NLSP case [26]. For generic parameter regions of the CMSSM, we show that this constraint disfavors $T_R > 10^7$ GeV and thereby successful thermal leptogenesis.

Entropy production after decoupling of the NLSP and before BBN can weaken the BBN constraints significantly [27]. At the same time, the gravitino density is diluted which relaxes the bounds on T_R . We show explicitly the effect of entropy production on the T_R bounds. Here we consider the cases of late-time entropy production before and after the decoupling of the NLSP. Indeed, a relaxation of the T_R bounds can render models of inflation with $T_R > 10^7$ GeV viable in CMSSM scenarios with gravitino dark matter. Since also a baryon asymmetry generated in the early Universe is diluted, the temperature required by thermal leptogenesis increases in a cosmological scenario with late-time entropy production. Still, we find that a sufficient amount of entropy production after NLSP decoupling and before BBN can revive successful thermal leptogenesis.

THERMAL GRAVITINO PRODUCTION

Gravitinos with $m_{\tilde{G}} \gtrsim 1$ GeV have decoupling temperatures of $T_{\tilde{G}}^{\tilde{G}} \gtrsim 10^{14}$ GeV, as will be shown below. We consider thermal gravitino production in the radiation-dominated epoch starting at $T_R < T_{\tilde{G}}^{\tilde{G}}$ assuming that inflation has diluted away any initial gravitino population.² For $T_R < T_{\tilde{G}}^{\tilde{G}}$, gravitinos are not in thermal equilibrium with the post-inflationary plasma. Accordingly, the evolution of the gravitino number density $n_{\tilde{G}}$ with cosmic time t is described by the following Boltzmann

TABLE I: The gauge couplings g_i , the gaugino mass parameters M_i , and the constants c_i , k_i , y_i , and $\beta_i^{(1)}$ associated with the gauge groups $U(1)_Y$, $SU(2)_L$, and $SU(3)_c$.

gauge group	i	g_i	M_i	c_i	k_i	$(y_i/10^{-12})$	$\beta_i^{(1)}$
$U(1)_Y$	1	g'	M_1	11	1.266	0.653	11
$SU(2)_L$	2	g	M_2	27	1.312	1.604	1
$SU(3)_c$	3	g_s	M_3	72	1.271	4.276	-3

equation [11]

$$\frac{dn_{\tilde{G}}}{dt} + 3Hn_{\tilde{G}} = C_{\tilde{G}} \quad (1)$$

$$C_{\tilde{G}} = \sum_{i=1}^3 \frac{3\zeta(3)T^6}{16\pi^3 M_{\text{P}}^2} \left(1 + \frac{M_i^2}{3m_{\tilde{G}}^2} \right) c_i g_i^2 \ln \left(\frac{k_i}{g_i} \right) \quad (2)$$

where H denotes the Hubble parameter. The collision term $C_{\tilde{G}}$ involves the gaugino mass parameters M_i , the gauge couplings g_i , and the constants c_i and k_i associated with the gauge groups $U(1)_Y$, $SU(2)_L$, and $SU(3)_c$ as given in Table I. In expression (2) the temperature T provides the scale for the evaluation of M_i and g_i . The given collision term is valid for temperatures sufficiently below the gravitino decoupling temperature, where gravitino disappearance processes can be neglected. A primordial plasma with the particle content of the minimal SUSY Standard Model (MSSM) in the high-temperature limit is used in the derivation of (2).

The collision term (2) results from a consistent gauge-invariant finite-temperature calculation [11, 18] following the approach used in Ref. [10]. Thus, in contrast to the previous estimates in [7, 8], the expression for $C_{\tilde{G}}$ is independent of arbitrary cutoffs. Note that the field-theoretical methods of [30, 31] applied in its derivation require weak couplings, $g_i \ll 1$, and thus high temperatures $T \gg 10^6$ GeV.

Assuming conservation of entropy per comoving volume, the Boltzmann equation (1) can be solved to good approximation analytically [10, 32]. At a temperature $T_{\text{low}} \ll T_R$, the resulting gravitino yield from thermal production reads

$$\begin{aligned} Y_{\tilde{G}}^{\text{TP}}(T_{\text{low}}) &\equiv \frac{n_{\tilde{G}}^{\text{TP}}(T_{\text{low}})}{s(T_{\text{low}})} \approx \frac{C_{\tilde{G}}(T_R)}{s(T_R) H(T_R)} \\ &= \sum_{i=1}^3 y_i g_i^2(T_R) \left(1 + \frac{M_i^2(T_R)}{3m_{\tilde{G}}^2} \right) \\ &\quad \times \ln \left(\frac{k_i}{g_i(T_R)} \right) \left(\frac{T_R}{10^{10} \text{ GeV}} \right), \quad (3) \end{aligned}$$

where the constants y_i are given in Table I. These constants are obtained with the Hubble parameter describing the radiation-dominated epoch, $H_{\text{rad}}(T) =$

² Taking a conservative point of view, we do not include gravitino production before the radiation-dominated epoch. However, inflaton decays, for example, can lead to a sizable yield of non-thermally produced gravitinos depending on the inflation model; cf. [28, 29] and references therein.

$\sqrt{g_*(T)\pi^2/90}T^2/M_{\text{P}}$, the entropy density $s(T) = 2\pi^2 g_{*S}(T)T^3/45$, and an effective number of relativistic degrees of freedom of $g_*(T_{\text{R}}) = g_{*S}(T_{\text{R}}) = 228.75$. We evaluate $g_i(T_{\text{R}})$ and $M_i(T_{\text{R}})$ using the one-loop evolution described by the renormalization group equation in the MSSM:

$$g_i(T) = \left(g_i^{-2}(m_Z) - \frac{\beta_i^{(1)}}{8\pi^2} \ln \left[\frac{T}{m_Z} \right] \right)^{-1/2}, \quad (4)$$

$$M_i(T) = \left[\frac{g_i(T)}{g_i(M_{\text{GUT}})} \right]^2 M_i(M_{\text{GUT}}) \quad (5)$$

with the respective gauge coupling at the Z-boson mass, $g_i(m_Z)$, and the $\beta_i^{(1)}$ coefficients listed in Table I.

Without late-time entropy production, the gravitino yield from thermal production at the present temperature T_0 is given by

$$Y_{\tilde{G}}^{\text{TP}}(T_0) = Y_{\tilde{G}}^{\text{TP}}(T_{\text{low}}). \quad (6)$$

The resulting density parameter of thermally produced gravitinos is

$$\Omega_{\tilde{G}}^{\text{TP}} h^2 = m_{\tilde{G}} Y_{\tilde{G}}^{\text{TP}}(T_0) s(T_0) h^2 / \rho_c \quad (7)$$

with the Hubble constant h in units of $100 \text{ km Mpc}^{-1} \text{ s}^{-1}$ and $\rho_c/[s(T_0)h^2] = 3.6 \times 10^{-9} \text{ GeV}$.

In Fig. 1 our result (3) for the thermally produced gravitino yield $Y_{\tilde{G}}^{\text{TP}}(T_{\text{low}})$ is shown as a function of T_{R} for various values of $m_{\tilde{G}}$ (solid lines). The curves are obtained with $m_{1/2} = 500 \text{ GeV}$ for the case of universal gaugino masses at M_{GUT} : $M_{1,2,3}(M_{\text{GUT}}) = m_{1/2}$. The dotted lines show the corresponding results from the $\text{SU}(3)_c$ yield of Ref. [10] for $M_3 = m_{1/2}$, which was used to study T_{R} constraints on gravitino dark matter scenarios in Refs. [13, 14, 15]. We find that (3) exceeds the yield derived from [10] by about 50%; cf. [11]. The dashed (blue in the web version) horizontal line indicates the equilibrium yield

$$Y_{\tilde{G}}^{\text{eq}} \equiv \frac{n_{\tilde{G}}^{\text{eq}}}{s} \approx 1.8 \times 10^{-3} \quad (8)$$

which is given by the equilibrium number density of a relativistic spin 1/2 Majorana fermion, $n_{\tilde{G}}^{\text{eq}} = 3\zeta(3)T^3/(2\pi^2)$. For $T > T_{\text{f}}^{\tilde{G}}$, $g_*(T) = g_{*S}(T) = 230.75$ since the spin 1/2 components of the gravitino are in thermal equilibrium. In the region where the yield (3) approaches the equilibrium value (8), gravitino disappearance processes should be taken into account. This would then lead to a smooth approach of the non-equilibrium yield to the equilibrium abundance. Without the back-reactions taken into account, the kink position indicates a lower bound for $T_{\text{f}}^{\tilde{G}}$. Towards smaller $m_{\tilde{G}}$, $T_{\text{f}}^{\tilde{G}}$ decreases due to the increasing strength of the gravitino couplings. For example, for $m_{\tilde{G}} = 1 \text{ GeV}$ (10 MeV), we find $T_{\text{f}}^{\tilde{G}} \gtrsim 10^{14} \text{ GeV}$ (10^{10} GeV).

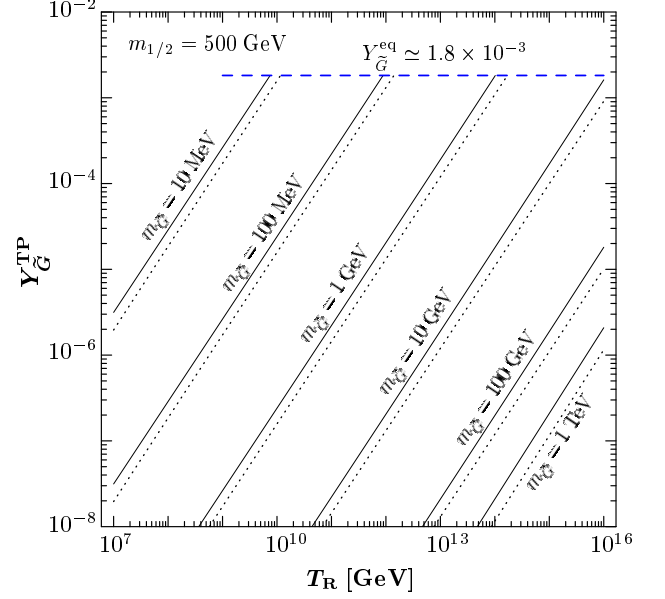


FIG. 1: The thermally produced gravitino yield (3) as a function of T_{R} for $m_{\tilde{G}} = 10 \text{ MeV}$, 100 MeV , 1 GeV , 10 GeV , 100 GeV , and 1 TeV (solid lines from left to right) and $M_{1,2,3}(M_{\text{GUT}}) = m_{1/2} = 500 \text{ GeV}$. The dotted lines show the corresponding yield obtained with the $\text{SU}(3)_c$ result for the collision term of Ref. [10]. The dashed (blue in the web version) horizontal line indicates the equilibrium yield of a relativistic spin 1/2 Majorana fermion.

In the analytical expression (3) we refer to T_{R} as the initial temperature of the radiation-dominated epoch. So far we have not considered the phase in which the coherent oscillations of the inflaton field ϕ dominate the energy density of the Universe, where one usually defines T_{R} in terms of the decay width Γ_{ϕ} of the inflaton field ϕ . To account for the reheating phase, we numerically integrate (1) together with the Boltzmann equations for the energy densities of radiation and the inflaton field,

$$\frac{d\rho_{\text{rad}}}{dt} + 4H\rho_{\text{rad}} = \Gamma_{\phi}\rho_{\phi}, \quad (9)$$

$$\frac{d\rho_{\phi}}{dt} + 3H\rho_{\phi} = -\Gamma_{\phi}\rho_{\phi}, \quad (10)$$

respectively; for details see Appendix F of Ref. [34].

With our result for the collision term (2), we find that the gravitino yield obtained numerically is in good agreement with the analytical expression (3) for

$$T_{\text{R}} \simeq \left[\frac{90}{g_*(T_{\text{R}})\pi^2} \right]^{1/4} \sqrt{\frac{\Gamma_{\phi} M_{\text{P}}}{1.8}} \quad (11)$$

which satisfies $\Gamma_{\phi} \simeq 1.8 H_{\text{rad}}(T_{\text{R}})$. For an alternative T_{R} definition given by $\Gamma_{\phi} = \xi H_{\text{rad}}(T_{\text{R}})$,

$$T_{\text{R}}^{\xi} \equiv \left[\frac{90}{g_*(T_{\text{R}})\pi^2} \right]^{1/4} \sqrt{\frac{\Gamma_{\phi} M_{\text{P}}}{\xi}}, \quad (12)$$

the associated numerically obtained gravitino yield is described by the analytical expression obtained after substituting T_R with $\sqrt{\xi/1.8}T_R^\xi$ in (3).

While we focus on scenarios in which the gravitino is stable, the yield (3) is also crucial to extract cosmological constraints in scenarios with unstable gravitinos. Based on the result of [10] and taking into account thermal gravitino production during reheating, the following fitting formula was used to study constraints from decaying gravitinos in Refs. [33, 34, 35]:

$$Y_{\tilde{G}}^{\text{KKM}}(T_{\text{low}}) \simeq 1.9 \times 10^{-12} \left(\frac{T_R}{10^{10} \text{ GeV}} \right) \times \left[1 + 0.045 \ln \left(\frac{T_R}{10^{10} \text{ GeV}} \right) \right] \times \left[1 - 0.028 \ln \left(\frac{T_R}{10^{10} \text{ GeV}} \right) \right], \quad (13)$$

where T_R was defined via $\Gamma_\phi = 3H_{\text{rad}}(T_R)$. Comparing (13) with our result after the matching of the T_R definitions, we find that our result exceeds the $m_{\tilde{G}}$ -independent yield (13) by about 30% for $m_{\tilde{G}} \gg M_i(T_R)$. While the $m_{\tilde{G}}$ dependence of $Y_{\tilde{G}}^{\text{TP}}$ becomes negligible for decreasing $M_i(T_R)/m_{\tilde{G}}$, the yield (13) is used for $m_{\tilde{G}}$ as small as 100 GeV in Refs. [33, 34, 35]. As can be seen in Fig. 1, the actual yield for $m_{\tilde{G}} = 100$ GeV is thereby underestimated by about an order of magnitude. Accordingly, the T_R bounds given in [33, 34, 35] are underestimated in the region $m_{\tilde{G}} < 1$ TeV.

CONSTRAINTS ON T_R

The reheating temperature T_R is limited from above in the case of a stable gravitino LSP since $\Omega_{\tilde{G}}^{\text{TP}}$ cannot exceed the dark matter density Ω_{dm} [8, 12, 13, 14, 15]. In this paper, we use [36, 37]

$$\Omega_{\text{dm}}^{3\sigma} h^2 = 0.105_{-0.030}^{+0.021} \quad (14)$$

as obtained from the measurements of the cosmic microwave background (CMB) anisotropies by the Wilkinson Microwave Anisotropy Probe (WMAP) satellite.³

In Fig. 2 we show the resulting upper limits on T_R as a function of $m_{\tilde{G}}$. On the gray band, the thermally produced gravitino density (7) is within the nominal 3σ range (14). The upper (lower) gray band is obtained for $M_{1,2,3} = m_{1/2}$ at M_{GUT} with $m_{1/2} = 500$ GeV (2 TeV). The dashed lines show the corresponding constraints for the exemplary non-universal scenario [39]

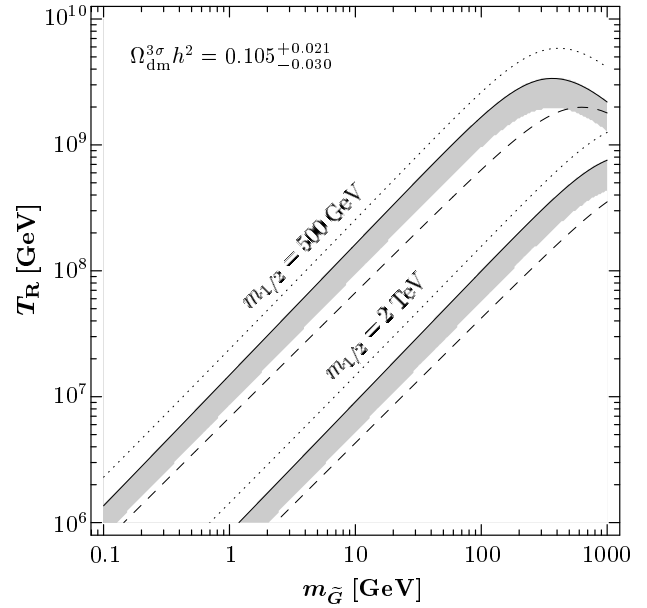


FIG. 2: Upper limits on the reheating temperature T_R . On the upper (lower) gray band, $\Omega_{\tilde{G}}^{\text{TP}}$ for $M_{1,2,3} = m_{1/2} = 500$ GeV (2 TeV) at M_{GUT} agrees with $\Omega_{\text{dm}}^{3\sigma}$. The corresponding T_R limits from the requirement $\Omega_{\tilde{G}}^{\text{TP}} h^2 \leq 0.126$ shown by the dashed and dotted lines are obtained respectively with (3) for $M_1/10 = M_2/2 = M_3 = m_{1/2}$ at M_{GUT} and with the result of Ref. [10] for $M_3 = m_{1/2}$ at M_{GUT} .

$M_1/10 = M_2/2 = M_3 = m_{1/2}$ at M_{GUT} and from the requirement $\Omega_{\tilde{G}}^{\text{TP}} h^2 \leq 0.126$. Using the same requirement and the result of [10] for $M_3 = m_{1/2}$, we obtain the dotted lines. The electroweak contributions are particularly important for the considered case of non-universal gaugino masses at M_{GUT} . For universal gaugino masses at M_{GUT} , the T_R limits derived with the result of [10] provide already reasonable estimates.⁴

The T_R limits shown in Fig. 2 are conservative bounds that do only depend on $m_{\tilde{G}}$ and the M_i values at M_{GUT} . Once details of the SUSY model realized in Nature are known, one will be able to refine the limits by including contributions to $\Omega_{\tilde{G}}$ from NLSP decays. In the next section, we will account for this non-thermal gravitino production in a systematic way within the framework of the CMSSM.

³ This nominal 3σ range is derived assuming a restrictive six-parameter “vanilla” model. A larger range is possible—even with additional data from other cosmological probes—if the fit is performed in the context of a more general model [38].

⁴ Note that the dotted curve shown for $m_{1/2} = 500$ GeV in Fig. 2 is by about a factor of 4 more severe than the T_R limits shown in Figs. 5 and 6 of Ref. [14] in the region $m_{\tilde{G}} \lesssim 10$ GeV in which $\Omega_{\tilde{G}}^{\text{TP}}$ governs the limits. It seems to us that the gluino mass in (1.2) of Ref. [14] was accidentally evaluated at the scale $\mu = T_R$ rather than at the scale $\mu \simeq 100$ GeV; see Sec. 5 of [10].

CONSTRAINTS ON T_R IN THE CMSSM

In the CMSSM, one assumes universal soft SUSY breaking parameters at M_{GUT} . The CMSSM yields phenomenologically acceptable spectra with only four parameters and a sign: the gaugino mass parameter $m_{1/2}$, the scalar mass parameter m_0 , the trilinear coupling A_0 , the mixing angle $\tan\beta$ in the Higgs sector, and the sign of the higgsino mass parameter μ .

Assuming $A_0 = 0$ for simplicity, the lightest Standard Model superpartner is either the lightest neutralino $\tilde{\chi}_1^0$ or the lighter stau $\tilde{\tau}_1$. Indeed, most CMSSM investigations assume that $\tilde{\chi}_1^0$ is the LSP that provides dark matter; cf. [40] and references therein. The parameter region in which $m_{\tilde{\tau}_1} < m_{\tilde{\chi}_1^0}$ is usually not considered because of the severe upper limits on the abundance of stable charged particles [37]. In the gravitino LSP case, $m_{\tilde{\tau}_1} < m_{\tilde{\chi}_1^0}$ can be viable since the lightest Standard Model superpartner is unstable [13, 14, 25, 41].

With the gravitino LSP, the lightest Standard Model superpartner is the NLSP that decays into Standard Model particles and one gravitino LSP. For $m_{\tilde{G}} \gtrsim 1$ GeV, the NLSP decays after its decoupling from the thermal plasma.⁵ Thus, the relic density of the associated non-thermally produced gravitinos reads [42]

$$\Omega_{\tilde{G}}^{\text{NTP}} h^2 = m_{\tilde{G}} Y_{\text{NLSP}}(T_0) s(T_0) h^2 / \rho_c \quad (15)$$

$$= \frac{m_{\tilde{G}}}{m_{\text{NLSP}}} \Omega_{\text{NLSP}} h^2, \quad (16)$$

where m_{NLSP} is the mass of the NLSP and $Y_{\text{NLSP}}(T_0)$ and $\Omega_{\text{NLSP}} h^2$ are respectively the yield and the relic density that the NLSP would have today, if it had not decayed.

In Fig. 3 the solid (black) and dotted (blue in the web version) lines show respectively contours of $Y_{\text{NLSP}}(T_0)$ and m_{NLSP} in the $(m_{1/2}, m_0)$ plane for $A_0 = 0$, $\mu > 0$, $\tan\beta = 10$ (left panel) and $\tan\beta = 30$ (right panel). Above (below) the dashed line, $m_{\tilde{\chi}_1^0} < m_{\tilde{\tau}_1}$ ($m_{\tilde{\tau}_1} < m_{\tilde{\chi}_1^0}$). The medium gray and the light gray regions at small $m_{1/2}$ are excluded respectively by the mass bounds $m_{\tilde{\chi}_1^\pm} > 94$ GeV and $m_H > 114.4$ GeV from chargino and Higgs searches at LEP [37]. The leftmost dotted (blue in the web version) line indicates the LEP bound $m_{\tilde{\tau}_1} > 81.9$ GeV [37]. For $\tan\beta = 30$, tachyonic sfermions occur in the low-energy spectrum at points in the white corner labeled as “tachyonic.” We employ the FORTRAN program **SuSpect** [43] to calculate the low-energy spectrum of the superparticles and the Higgs bosons, where we use $m_t = 172.5$ GeV for the top quark mass. Assuming standard cosmology, the yield $Y_{\text{NLSP}}(T_0)$ is obtained

from the $\Omega_{\text{NLSP}} h^2$ values provided by the computer program **micrOMEGAs** [44].

The contours shown in Fig. 3 are independent of $m_{\tilde{G}}$ and T_R . Therefore, they can be used to interpret the results shown in the figures below. Note the sensitivity of both $Y_{\tilde{\tau}_1}(T_0)$ and $m_{\tilde{\tau}_1}$ on $\tan\beta$. By going from $\tan\beta = 10$ to $\tan\beta = 30$, $Y_{\tilde{\tau}_1}(T_0)$ decreases by about a factor of two at points that are not in the vicinity of the dashed line, i.e., that are outside of the $\tilde{\tau}_1 - \tilde{\chi}_1^0$ coannihilation region. While $m_{\tilde{\tau}_1}$ becomes smaller by increasing $\tan\beta$ to 30, the $\tan\beta$ dependence of $m_{\tilde{\chi}_1^0}$ is negligible.

Let us now explore the parameter space in which

$$0.075 \leq \Omega_{\tilde{G}}^{\text{TP}} h^2 + \Omega_{\tilde{G}}^{\text{NTP}} h^2 \leq 0.126. \quad (17)$$

Now, T_R and $m_{\tilde{G}}$ appear in addition to the traditional CMSSM parameters. We focus on $m_{\tilde{G}} \gtrsim 1$ GeV since the soft SUSY breaking parameters of the CMSSM are usually assumed to result from gravity-mediated SUSY breaking. However, we do not restrict our study to fixed relations between $m_{\tilde{G}}$ and the soft SUSY breaking parameters such as the ones suggested, for example, by the Polonyi model.

In Fig. 4 the light, medium, and dark shaded (green in the web version) bands show the $(m_{1/2}, m_0)$ regions that satisfy the constraint (17) for $T_R = 10^7, 10^8$, and 10^9 GeV, respectively, where $\tan\beta = 10$, $A_0 = 0$, $\mu > 0$. The four panels are obtained for the choices (a) $m_{\tilde{G}} = 10$ GeV, (b) $m_{\tilde{G}} = 100$ GeV, (c) $m_{\tilde{G}} = 0.2 m_0$, and (d) $m_{\tilde{G}} = m_0$. In the dark-gray region, the gravitino is not the LSP. The regions excluded by the chargino and Higgs mass bounds and the line indicating $m_{\tilde{\chi}_1^0} = m_{\tilde{\tau}_1}$ are identical to the ones shown in the left panel of Fig. 3. The dotted lines show contours of the NLSP lifetime. For the $\tilde{\tau}_1$ NLSP,

$$\tau_{\tilde{\tau}_1} \simeq \Gamma^{-1}(\tilde{\tau}_1 \rightarrow \tilde{G}\tau) = \frac{48\pi m_{\tilde{G}}^2 M_{\text{P}}^2}{m_{\tilde{\tau}_1}^5} \left(1 - \frac{m_{\tilde{G}}^2}{m_{\tilde{\tau}_1}^2}\right)^{-4} \quad (18)$$

as obtained in the limit $m_\tau \rightarrow 0$. For the $\tilde{\chi}_1^0$ NLSP, we calculate $\tau_{\tilde{\chi}_1^0}$ from the expressions given in Sec. IIC of Ref. [21].

The τ_{NLSP} contours in Fig. 4 illustrate that the NLSP decays during/after BBN. Successful BBN predictions therefore imply cosmological constraints on $m_{\tilde{G}}$, m_{NLSP} , and Y_{NLSP} [13, 14, 15, 21]. Indeed, it has been found that the considered $\tilde{\chi}_1^0$ NLSP region is completely disfavored for $m_{\tilde{G}} \gtrsim 1$ GeV by constraints from late electromagnetic and hadronic energy injection [13, 14, 21, 25]. In the $\tilde{\tau}_1$ NLSP region, the constraints from electromagnetic and hadronic energy release are important but far less severe than in the $\tilde{\chi}_1^0$ NLSP case. Thus, much of the $\tilde{\tau}_1$ NLSP region was believed to be cosmologically allowed [13, 14, 15, 21].

Recently, this picture has changed. It has been found that bound-state formation of long-lived negatively

⁵ The NLSP freezeout temperature can be estimated from its mass: $T_{\text{f}}^{\text{NLSP}} \lesssim m_{\text{NLSP}}/20$ [12]. Thus, $T_R \gg T_{\text{f}}^{\text{NLSP}}$ for $T_R > 10^6$ GeV which is considered in this Letter.

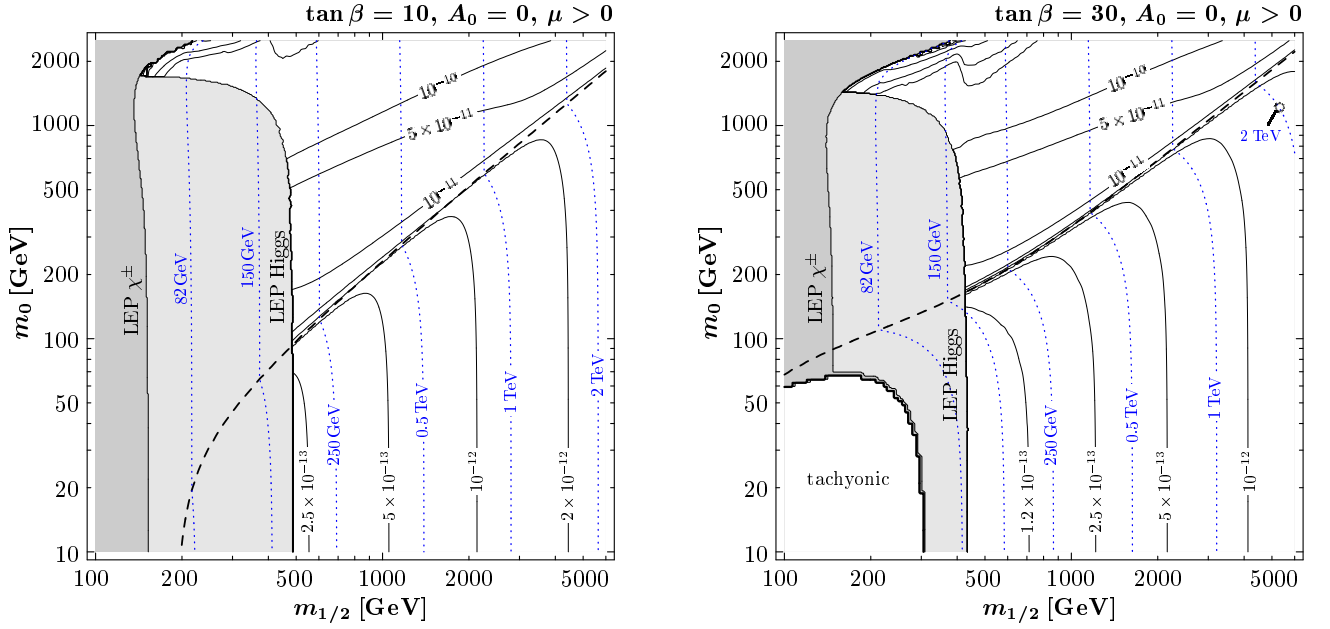


FIG. 3: Contours of $Y_{\text{NLSP}}(T_0)$ (solid black lines) and m_{NLSP} (dotted blue lines) in the $(m_{1/2}, m_0)$ plane for $A_0 = 0$, $\mu > 0$, $\tan \beta = 10$ (left panel) and $\tan \beta = 30$ (right panel). Above (below) the dashed line, $m_{\tilde{\chi}_1^0} < m_{\tilde{\tau}_1}$ ($m_{\tilde{\tau}_1} < m_{\tilde{\chi}_1^0}$). The medium gray and the light gray regions at small $m_{1/2}$ show the mass bounds $m_{\tilde{\chi}_1^\pm} > 94$ GeV and $m_H > 114.4$ GeV from chargino and Higgs searches at LEP [37].

charged $\tilde{\tau}_1$'s with primordial nuclei can catalyze the production of ${}^6\text{Li}$ significantly [22, 25]. Indeed, in most of the $\tilde{\tau}_1$ NLSP parameter space, the associated bounds are much more severe than the ones from late energy injection. Only for $\tau_{\tilde{\tau}_1} \lesssim 10^3$ s and $m_{\tilde{G}} \gtrsim 40$ GeV, the constraints from hadronic energy release can become more severe than the ones from catalyzed ${}^6\text{Li}$ production [25, 26]. We thus consider both the constraint from catalyzed ${}^6\text{Li}$ production derived in [22] and the one from late hadronic energy injection derived in [15].⁶

For the constraint from bound-state effects on ${}^6\text{Li}$ production, we adopt the bounds given in Fig. 4 of Ref. [22] as $\tau_{\tilde{\tau}_1}$ -dependent upper limits on the yield of the negatively charged staus, $Y_{\text{NLSP}}/2$. These bounds are obtained assuming a limiting primordial abundance of [45]

$$({}^6\text{Li}/\text{H})_{\text{p}} \lesssim 2 \times 10^{-11}. \quad (19)$$

The resulting constraint disfavors the $\tilde{\tau}_1$ NLSP region to the left of the long-dash-dotted (red in the web version) line shown in Fig. 4.

For the constraint from late hadronic energy injection, we use the upper limits on Y_{NLSP} that are given in Fig. 11 of Ref. [15]. These limits are derived from a computation

of the 4-body decay of the stau NLSP into the gravitino, the tau, and a quark-antiquark pair.⁷ They are based on the severe and conservative upper bounds on the released hadronic energy (95% CL) obtained in [34] for observed values of the primordial D abundance of

$$\begin{aligned} (n_{\text{D}}/n_{\text{H}})_{\text{mean}} &= (2.78^{+0.44}_{-0.38}) \times 10^{-5} \quad (\text{severe}), \\ (n_{\text{D}}/n_{\text{H}})_{\text{high}} &= (3.98^{+0.59}_{-0.67}) \times 10^{-5} \quad (\text{conservative}). \end{aligned}$$

In Fig. 4 the associated constraints are shown by the short-dash-dotted (blue in the web version) lines. The D constraint disfavors the region between the corresponding lines in panel (b) and the region above the corresponding lines in panels (c) and (d). In panel (a) the D constraint does not appear.⁸

Remarkably, one finds in each panel of Fig. 4 that the highest T_{R} value allowed by the considered BBN constraints is about 10^7 GeV. The bands obtained for $T_{\text{R}} \gtrsim 10^8$ GeV are located completely within the region

⁶ For details on the other BBN bounds and the additional CMB bounds, we refer the reader to the detailed investigations presented in Refs. [13, 14, 21, 41, 46].

⁷ The 3-body estimate of the hadronic energy release given in Ref. [21] leads to overly restrictive limits, as shown in Ref. [15].

⁸ Additional constraints on hadronic energy release are imposed by the primordial abundances of ${}^4\text{He}$, ${}^3\text{He}/\text{D}$, ${}^7\text{Li}$, and ${}^6\text{Li}/{}^7\text{Li}$ [25, 34, 47, 48, 49, 50]. However, in the region allowed by the ${}^6\text{Li}$ constraint from bound-state effects, i.e., $\tau_{\tilde{\tau}_1} \lesssim 10^3$ s, the considered D constraint on hadronic energy release is the dominant one as can be seen in Figs. 38–41 of Ref. [34] and Figs. 6–8 of Ref. [50].

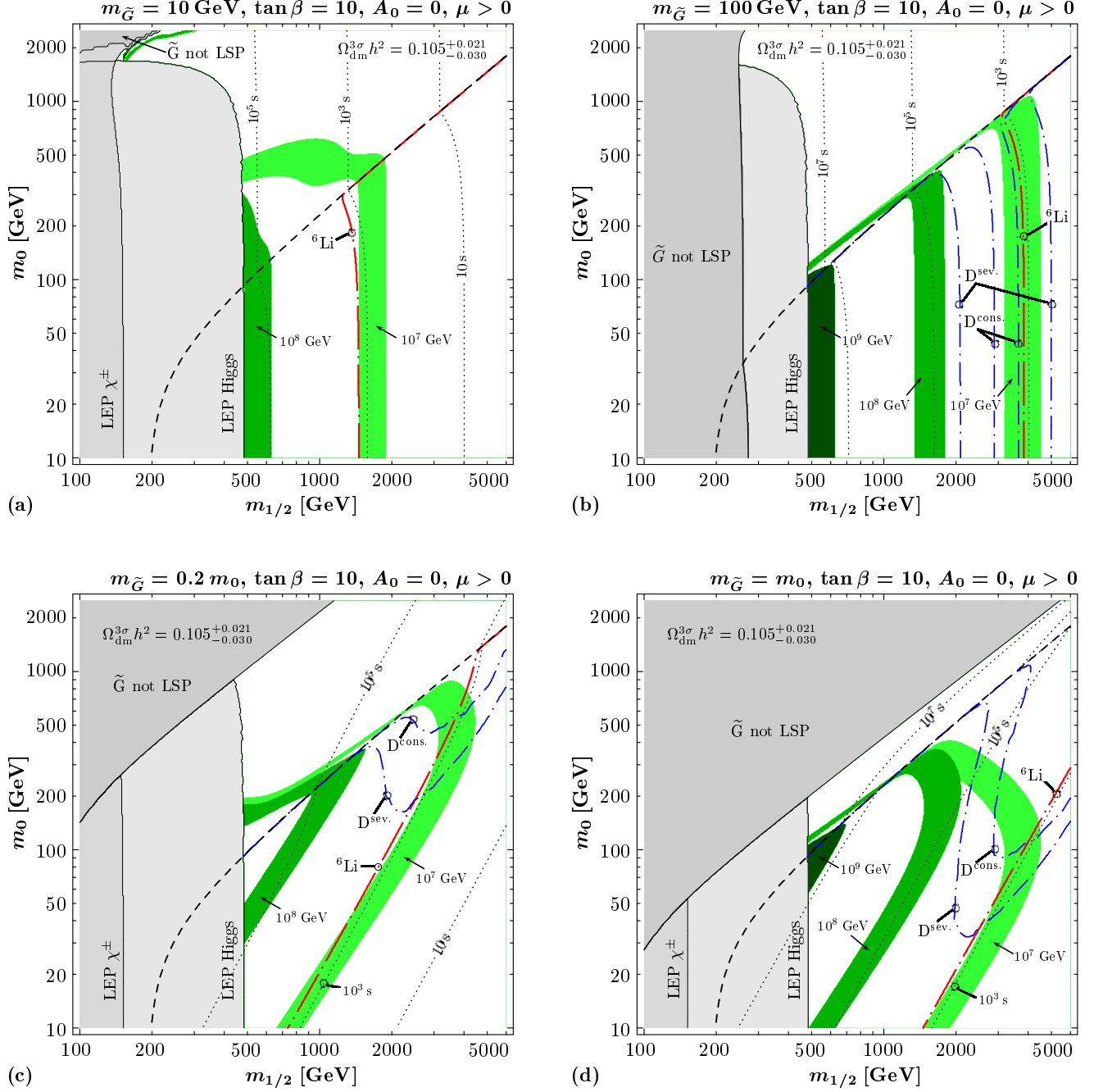


FIG. 4: The $(m_{1/2}, m_0)$ planes for $\tan \beta = 10$, $A_0 = 0$, $\mu > 0$, and the choices (a) $m_{\tilde{G}} = 10$ GeV, (b) $m_{\tilde{G}} = 100$ GeV, (c) $m_{\tilde{G}} = 0.2 m_0$, and (d) $m_{\tilde{G}} = m_0$. In each panel, the light, medium, and dark shaded (green in the web version) bands indicate the regions in which $0.075 \leq \Omega_{\tilde{G}} h^2 \leq 0.126$ for $T_R = 10^7$, 10^8 , and 10^9 GeV, respectively. The medium gray and the light gray regions at small $m_{1/2}$ are excluded respectively by chargino and Higgs searches at LEP. In the dark gray region, the gravitino is not the LSP. The dotted lines show contours of the NLSP lifetime. Below the dashed line, $m_{\tilde{\tau}_1} < m_{\tilde{\chi}_1^0}$. With the $\tilde{\tau}_1$ NLSP, the region to the left of the long-dash-dotted (red in the web version) line is cosmologically disfavored by bound-state effects on the primordial ${}^6\text{Li}$ abundance [22]. The effects of late hadronic energy injection on the primordial D abundance [15] disfavor the $\tilde{\tau}_1$ NLSP region between the short-dash-dotted (blue in the web version) lines in panel (b) and the one above the corresponding lines in panels (c) and (d). The $\tilde{\chi}_1^0$ NLSP region above the dashed line, in which $m_{\tilde{\chi}_1^0} < m_{\tilde{\tau}_1}$, is cosmologically disfavored by the effects of late electromagnetic/hadronic energy injection on the abundances of the light primordial elements [13, 14, 21, 25, 41].

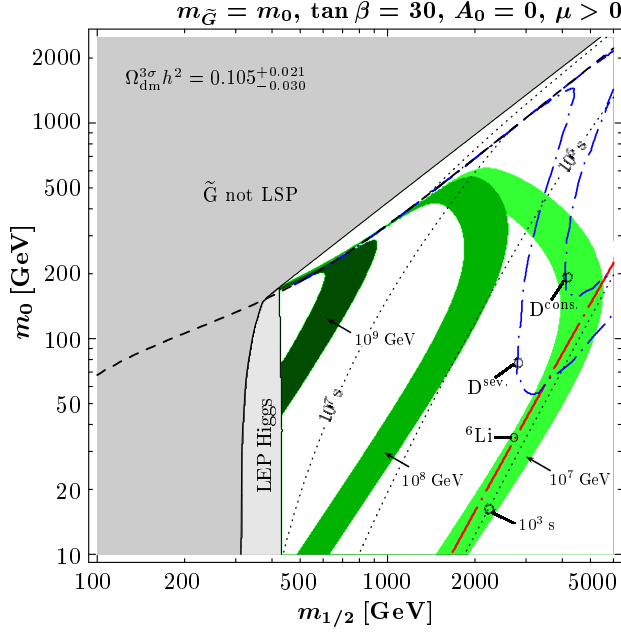


FIG. 5: As in Fig. 4 (d), for $\tan \beta = 30$, $A_0 = 0$, $\mu > 0$, and $m_{\tilde{G}} = m_0$.

disfavored by the ${}^6\text{Li}$ bound. In previous gravitino dark matter studies within the CMSSM that did not take into account bound-state effects on the primordial ${}^6\text{Li}$ abundance, much higher temperatures of up to about 10^9 GeV were believed to be allowed [11, 13, 14].⁹

The constraint $T_R \lesssim 10^7$ GeV remains if we consider larger values of $\tan \beta$. This is demonstrated in Fig. 5 for $\tan \beta = 30$, $A_0 = 0$, $\mu > 0$, and $m_{\tilde{G}} = m_0$. The shadings (colors in the web version) and line styles are identical to the ones in Fig. 4.

Let us comment on the dependence of the considered BBN constraints on the assumed primordial abundances of D and ${}^6\text{Li}$. As can be seen in Figs. 4 and 5, the constraint from late hadronic energy release is quite sensitive on the assumed primordial D abundance. In contrast, even if we relax the restrictive ${}^6\text{Li}$ bound on $Y_{\text{NLSP}}/2$ by two orders of magnitude, we still find $T_R \lesssim 10^7$ GeV. For example, the ${}^6\text{Li}$ constraint relaxed in this way would appear in Fig. 4 (b) as an almost vertical line slightly above $m_{1/2} = 3$ TeV.

While the constraint $T_R \lesssim 10^7$ GeV is found for each of the considered $m_{\tilde{G}}$ relations, one cannot use the ${}^6\text{Li}$ bound to set bounds on $m_{\tilde{\tau}_1}$ without insights into $m_{\tilde{G}}$. The ${}^6\text{Li}$ bound disappears for $\tau_{\tilde{\tau}_1} \lesssim 10^3$ s [22] which is possible even for $m_{\tilde{\tau}_1} = \mathcal{O}(100 \text{ GeV})$ provided $m_{\tilde{G}}$ is sufficiently small; see (18). However, the constraints on

T_R become more severe towards small $m_{\tilde{G}}$ as is shown in Fig. 2. Thus, the constraint $T_R \lesssim 10^7$ GeV cannot be evaded by lowering $m_{\tilde{G}}$ provided $T_R < T_f^{\tilde{G}}$.

An upper limit on T_R of 10^7 GeV can be problematic for inflation models and baryogenesis scenarios. This finding can thus be important for our understanding of the thermal history of the Universe.

CONSTRAINTS ON T_R WITH LATE-TIME ENTROPY PRODUCTION

The constraints shown above are applicable for a standard thermal history during the radiation-dominated epoch. However, it is possible that a substantial amount of entropy is released, for example, in out-of-equilibrium decays of a long-lived massive particle species X [2, 51].¹⁰

If X lives sufficiently long, it might decay while its rest mass dominates the energy density of the Universe. The associated evolution of the entropy per comoving volume, $S \equiv s a^3$, is described by [2, 51]

$$\frac{dS}{dt} = \frac{\Gamma_X \rho_X a^3}{T} = \left(\frac{2\pi^2}{45} g_* \right)^{1/3} \Gamma_X \rho_X a^4 S^{-1/3} \quad (20)$$

together with the Boltzmann equation (10) for $\phi = X$ and the Friedmann equation governing the evolution of the scale factor of the Universe a . Here Γ_X and ρ_X denote respectively the decay width and the energy density of X. Thus, the temperature after the decay can be expressed in terms of Γ_X ,

$$T_{\text{after}} \equiv \left[\frac{10}{g_*(T_{\text{after}})\pi^2} \right]^{1/4} \sqrt{\Gamma_X M_{\text{P}}} , \quad (21)$$

which satisfies $\Gamma_X = 3H_{\text{rad}}(T_{\text{after}})$. Indeed, primordial nucleosynthesis imposes a lower limit on this temperature [55, 56, 57, 58]:

$$T_{\text{after}} \gtrsim 0.7 - 4 \text{ MeV} . \quad (22)$$

In Fig. 6 we show the evolution of S , $a^3 \rho_X$, and $a^3 \rho_{\text{rad}}$ for two exemplary scenarios respecting (22). The scale factor a is normalized by $a_I \equiv a(10 \text{ GeV}) = 1 \text{ GeV}^{-1}$ and the temperature dependence of g_* is taken into account as determined in [59]. For $\rho_X(10 \text{ GeV}) = 0.1 \rho_{\text{rad}}(10 \text{ GeV})$ and $T_{\text{after}} = 6 \text{ MeV}$, S increases by a factor of $\Delta = 100$ as shown by the corresponding solid line. For $\rho_X(10 \text{ GeV}) = 8 \rho_{\text{rad}}(10 \text{ GeV})$ and $T_{\text{after}} = 4.9 \text{ MeV}$, S increases by a factor of $\Delta = 10^4$ as shown by the corresponding dotted (blue in the web version) line.

⁹ Note that our bands for $T_R = 10^9$ GeV differ from the ones shown in Refs. [13, 14]; see footnote 4.

¹⁰ Gravitino dark matter scenarios with late-time entropy production have been considered previously for gauge-mediated SUSY breaking where $T_R > T_f^{\tilde{G}}$ [52, 53, 54].

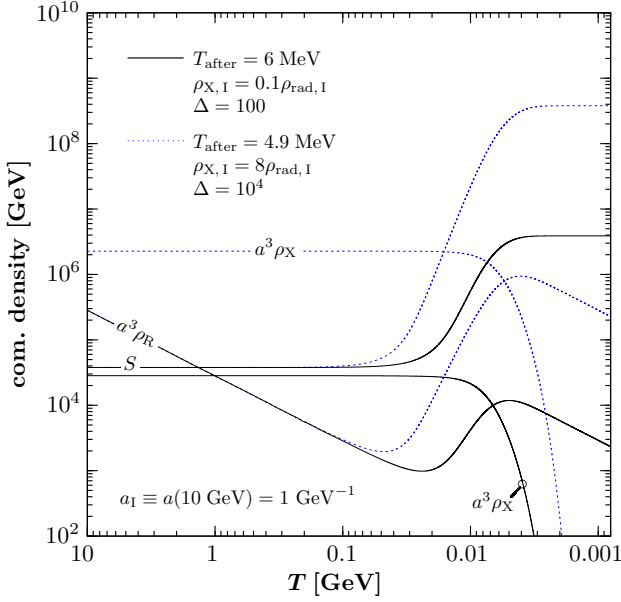


FIG. 6: Evolution of S , $a^3 \rho_X$, and $a^3 \rho_{\text{rad}}$ as a function of T for the normalization $a_I \equiv a(10 \text{ GeV}) = 1 \text{ GeV}^{-1}$. The solid lines are obtained for $\rho_X(10 \text{ GeV}) = 0.1 \rho_{\text{rad}}(10 \text{ GeV})$ and $T_{\text{after}} = 6 \text{ MeV}$, the dotted (blue in the web version) lines for $\rho_X(10 \text{ GeV}) = 8 \rho_{\text{rad}}(10 \text{ GeV})$ and $T_{\text{after}} = 4.9 \text{ MeV}$.

We restrict our study to entropy production at late times, $T_{\text{before}} \simeq T_{\text{low}} \ll T_R$, so that the thermal production of gravitinos is not affected. To work in a model independent way, we assume that the production of gravitinos and NLSPs in the entropy producing event, such as the direct production in decays of X , is negligible.¹¹ Moreover, in this section, we focus on scenarios in which the decoupling of the NLSP is not or at most marginally affected by entropy production, i.e., either $T_R \gg T_{\text{after}} \gg T_{\text{f}}^{\text{NLSP}}$ or $\rho_{\text{rad}} \gg \rho_X$ for $T \gtrsim T_{\text{f}}^{\text{NLSP}}$. Thus, the thermally produced gravitino yield and—in the case of entropy production after NLSP decoupling—also the non-thermally produced gravitino yield are diluted:

$$Y_{\tilde{G}}(T_{\text{after}}) = \frac{S(T_{\text{low}})}{S(T_{\text{after}})} Y_{\tilde{G}}(T_{\text{low}}). \quad (23)$$

In the case of late-time entropy production *before* the decoupling of the NLSP, we parameterize this by writing

$$Y_{\tilde{G}}^{\text{TP}}(T_0) = \frac{1}{\delta} Y_{\tilde{G}}^{\text{TP}}(T_{\text{low}}). \quad (24)$$

In this case, $Y_{\text{NLSP}}(T_0)$ and thereby $\Omega_{\tilde{G}}^{\text{NTP}}$ and the BBN constraints remain unaffected.

Conversely, in the case of late-time entropy production *after* the decoupling of the NLSP (and before BBN) both, $Y_{\tilde{G}}^{\text{TP}}(T_0)$ and $Y_{\text{NLSP}}(T_0)$, are reduced:

$$\begin{aligned} Y_{\tilde{G}}^{\text{TP}}(T_0) &= \frac{1}{\Delta} Y_{\tilde{G}}^{\text{TP}}(T_{\text{low}}) \\ Y_{\text{NLSP}}(T_0) &= \frac{1}{\Delta} Y_{\text{NLSP}}(T_{\text{low}}) \end{aligned} \quad (25)$$

Accordingly, $\Omega_{\tilde{G}}^{\text{TP}}$ and $\Omega_{\tilde{G}}^{\text{NTP}}$ become smaller and the BBN constraints can be relaxed.

In Fig. 7 we show how late-time entropy production before (left) and after (right) NLSP decoupling affects the ${}^6\text{Li}$ constraint and the region in which $0.075 \leq \Omega_{\tilde{G}} h^2 \leq 0.126$ for $T_R = 10^9 \text{ GeV}$. The $(m_{1/2}, m_0)$ planes are considered for $\tan \beta = 10$, $A_0 = 0$, $\mu > 0$, $m_{\tilde{G}} = 100 \text{ GeV}$ (upper panels) and $m_{\tilde{G}} = m_0$ (lower panels). The dark shaded (green in the web version) region is obtained without late time entropy production, $\delta = \Delta = 1$. The medium and light shaded (green in the web version) bands are obtained with a dilution of $\Omega_{\tilde{G}}^{\text{TP}}$ ($\Omega_{\tilde{G}}^{\text{TP}} + \Omega_{\tilde{G}}^{\text{NTP}}$) by $\delta = 10$ ($\Delta = 10$) and $\delta = 100$ ($\Delta = 100$), respectively. The dot-dashed (red in the web version) line illustrates that the ${}^6\text{Li}$ bound is independent of δ , as shown in the panels on the left-hand side, and becomes weaker (i.e., moves to the left) with increasing Δ , as shown in the panels on the right-hand side. Other curves and regions are identical to the ones in the corresponding panels of Fig. 4. Note that we do not show the D constraint on late hadronic energy injection since it is not sensitive to δ and vanishes already for $\Delta = 10$; an exception is the severe D constraint which still appears for $\Delta = 10$ in panel (d). BBN constraints on $\tilde{\chi}_1^0$ NLSP scenarios with entropy production after NLSP decoupling will be studied elsewhere.

Comparing panels (b) and (d) of Fig. 4 with panels (a) and (c) in Fig. 7, we find that a dilution factor of $\delta = 10$ (100) relaxes the T_R bound by a factor of 10 (100). Since the BBN constraints are unaffected by δ , the cosmologically disfavored range of NLSP masses cannot be relaxed. With the dilution after NLSP decoupling, the relaxation of the T_R constraints is more pronounced. Here also the cosmologically disfavored range of NLSP masses can be relaxed [27]. However, as can be seen in panels (b) and (d) of Fig. 7, the ${}^6\text{Li}$ bound is persistent. With a dilution factor of $\Delta = 100$, large regions of the $(m_{1/2}, m_0)$ plane remain cosmologically disfavored. For $\Delta \gtrsim 10^4$, however, the ${}^6\text{Li}$ bound can be evaded as will be shown explicitly below.

Figure 7 shows that inflation models predicting, for example, $T_R = 10^9 \text{ GeV}$ become allowed in the CMSSM with gravitino dark matter for $\delta = \Delta \approx 100$. Here it is not necessary to have late-time entropy production in the somewhat narrow window between NLSP decoupling and BBN. This is different for the viability of thermal leptogenesis in the considered scenarios ($T_{\text{f}}^{\tilde{G}} > T_R$) and for collider prospects as discussed below.

¹¹ The constraints discussed below shall therefore be considered as conservative bounds. For studies of gravitino production during an entropy producing event, we refer to [60] and references therein.

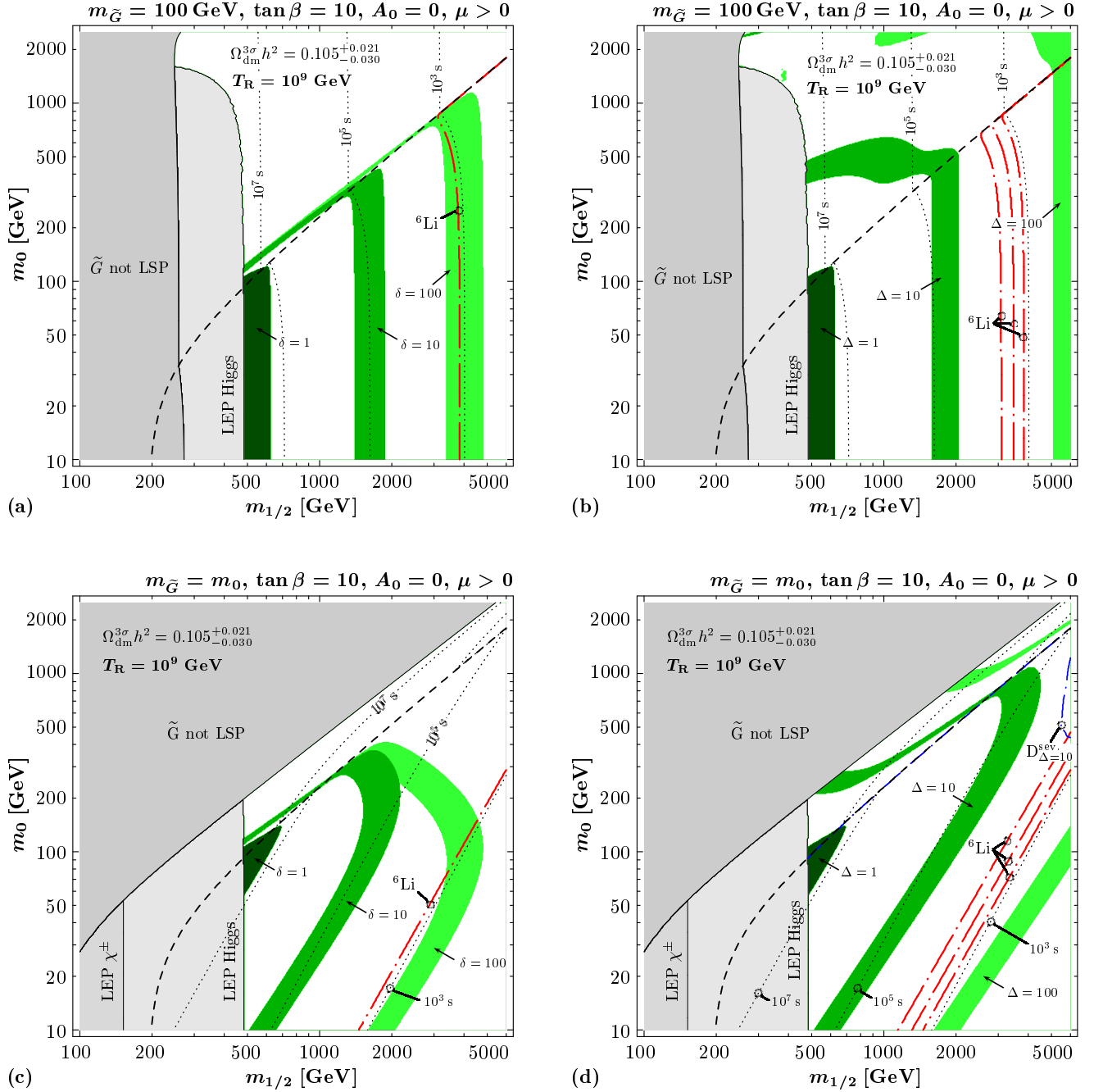


FIG. 7: The effect of late-time entropy production before (left) and after (right) NLSP decoupling on regions in which $0.075 \leq \Omega_{\tilde{G}} h^2 \leq 0.126$ for $T_R = 10^9$ GeV. The $(m_{1/2}, m_0)$ plane is shown for $\tan \beta = 10$, $A_0 = 0$, $\mu > 0$, $m_{\tilde{G}} = 100$ GeV (upper panels) and $m_{\tilde{G}} = m_0$ (lower panels). The dark shaded (green in the web version) region is obtained without late-time entropy production $\delta = \Delta = 1$. The medium and light shaded (green in the web version) bands are obtained with a dilution of $\Omega_{\tilde{G}}^{\text{TP}}$ ($\Omega_{\tilde{G}}^{\text{TP}} + \Omega_{\tilde{G}}^{\text{NTP}}$) by $\delta = 10$ ($\Delta = 10$) and $\delta = 100$ ($\Delta = 100$), respectively. The $\tilde{\tau}_1$ NLSP region to the right of the dot-dashed (red in the web version) line is cosmologically disfavored by the primordial ${}^6\text{Li}$ abundance. Other curves and regions are identical to the ones in the corresponding panels of Fig. 4. The severe D constraint for $\Delta = 10$ appears only in panel (d).

THERMAL LEPTOGENESIS IN THE CMSSM WITH GRAVITINO DARK MATTER

The constraint $T_R \lesssim 10^7$ GeV obtained in the considered CMSSM scenarios for a standard cosmological his-

tory strongly disfavors thermal leptogenesis. However, if entropy is released after NLSP decoupling, a dilution factor of $\Delta \simeq 10^4$ can render thermal leptogenesis viable for $T_R \simeq 10^{13}$ GeV.

Standard thermal leptogenesis usually requires $T_R \gtrsim 10^9$ GeV [17]. However, late-time entropy production dilutes the baryon asymmetry which is generated well before NLSP decoupling,

$$\eta(T_{\text{after}}) = \frac{1}{\Delta} \eta(T_{\text{before}}). \quad (26)$$

Therefore, the baryon asymmetry before entropy production must be larger by a factor of Δ in order to compensate for the dilution. For $\Delta \simeq 10^4$, this can be achieved in the case of hierarchical neutrinos for $M_{R1} \sim T_R \simeq 10^{13}$ GeV, as can be seen in Fig. 7 (a) of Ref. [61] and in Fig. 2 of Ref. [62]. Here M_{R1} is the mass of the lightest among the heavy right-handed Majorana neutrinos.

In Fig. 6 the dotted (blue in the web version) lines show a scenario in which a dilution factor of $\Delta = 10^4$ is generated in the out-of-equilibrium decay of a heavy particle X. Because of $\rho_X(10 \text{ GeV}) = 8 \rho_{\text{rad}}(10 \text{ GeV})$, the Hubble rate can be enhanced already during the decoupling phase of the NLSP, which leads to an increase of T_f^{NLSP} and $Y_{\text{NLSP}}(T_f^{\text{NLSP}})$. In the results shown below, we account for this by using a modified version of the **micrOMEGAs** code.¹² After entropy production, the net effect is still a significant reduction of $Y_{\text{NLSP}}(T_0)$. For the same initial conditions, $\Delta = 2 \times 10^4$ —and thereby an additional reduction of $Y_{\text{NLSP}}(T_0)$ by a factor of two—can be achieved by lowering T_{after} from 4.9 MeV down to 2.5 MeV.

We consider these two scenarios for $\tan \beta = 30$, $A_0 = 0$, $\mu > 0$, and $m_{\tilde{G}} = m_0$, in Fig. 8. Here the shaded (green in the web version) bands indicate the region in which $0.075 \leq \Omega_{\tilde{G}} h^2 \leq 0.126$ for $T_R = 10^{13}$ GeV and $\Delta = 10^4$ (dark) and 2×10^4 (medium). In addition, the corresponding evolution of the ${}^6\text{Li}$ bound is shown by the dot-dashed (red in the web version) lines. For $\Delta = 10^4$, the regions below the associated two rightmost curves and to the right of the associated leftmost curve are allowed. For $\Delta = 2 \times 10^4$, the cosmologically allowed region is the $\tilde{\tau}_1$ NLSP region below the line labeled accordingly. The gray regions are identical to the ones in Fig. 5.

We find that the ${}^6\text{Li}$ bound cannot be evaded for the $\tan \beta = 10$ scenarios even for $\Delta = 2 \times 10^4$ since $Y_{\text{NLSP}}(T_0)$ becomes larger. However, the ${}^6\text{Li}$ bound given in Fig. 4 of Ref. [22] depends linearly¹³ on the assumed limiting primordial abundance (19) that is subject to uncertainties; cf. Ref. [50]. Accordingly, for a limiting abundance that is a factor of two above the value given in (19), one obtains the ${}^6\text{Li}$ bound labeled with $\Delta = 2 \times 10^4$ in Fig. 8 for the scenario with $\tan \beta = 30$ and $\Delta = 10^4$.

Scenarios with successful thermal leptogenesis in the $\tilde{\tau}_1$ NLSP region are located preferably on the dark-shaded

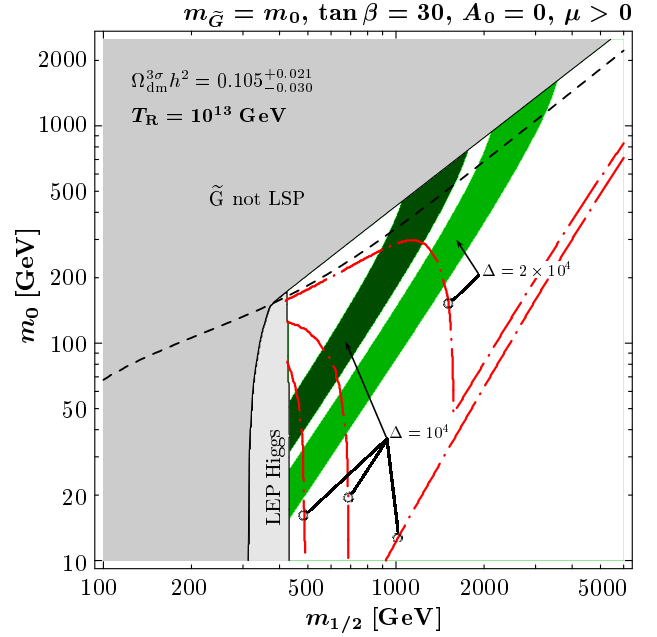


FIG. 8: The effect of entropy production after NLSP decoupling for $T_R = 10^{13}$ GeV and $\Delta \geq 10^4$ in the $(m_{1/2}, m_0)$ plane for $\tan \beta = 30$, $A_0 = 0$, $\mu > 0$, and $m_{\tilde{G}} = m_0$. The shaded (green in the web version) bands show the region in which $0.075 \leq \Omega_{\tilde{G}} h^2 \leq 0.126$ for $\Delta = 10^4$ (dark) and 2×10^4 (medium). The dot-dashed (red in the web version) lines illustrate the corresponding evolution of the ${}^6\text{Li}$ bound. For $\Delta = 10^4$, the regions below the associated two rightmost curves and to the right of the associated leftmost curve are allowed. For $\Delta = 2 \times 10^4$, the region below the line labeled accordingly is cosmologically allowed.

(dark green in the web version) band and in the white corner to its left, in which even slightly higher values of T_R are possible for $\Delta = 10^4$. For $T_R = 10^{13}$ GeV and $\Delta \gg 10^4$, the generated baryon asymmetry is diluted too strongly in order to explain the observed baryon asymmetry.

As can be seen in Fig. 8, the $\tilde{\tau}_1$ NLSP region with $500 \text{ GeV} \lesssim m_{1/2} \lesssim 700 \text{ GeV}$, where $m_{\tilde{\tau}_1} \lesssim 200 \text{ GeV}$ (cf. Fig. 3), is no longer disfavored by the ${}^6\text{Li}$ bound provided $\Delta \gtrsim 10^4$. Such scenarios are particularly promising since the long-lived $\tilde{\tau}_1$ NLSP could provide striking signatures of gravitino dark matter at future colliders [63, 64, 65, 66].

CONCLUSION

Using the full gauge-invariant result for $\Omega_{\tilde{G}}^{\text{TP}}$ to leading order in the Standard Model gauge couplings [11], we have studied bounds on T_R from the constraint $\Omega_{\tilde{G}} \leq \Omega_{\text{dm}}$. Our results take into account the dependence of $\Omega_{\tilde{G}}^{\text{TP}}$ on the masses of the gauginos associated with the

¹² The Y_{NLSP} contours shown in Fig. 3 do not apply in this section.

¹³ We thank M. Pospelov for bringing this point to our attention.

Standard Model gauge group $SU(3)_c \times SU(2)_L \times U(1)_Y$. This has allowed us to explore the dependence of the T_R bounds on the gaugino-mass relation at the scale of grand unification M_{GUT} .

Within the CMSSM, we have explored gravitino dark matter scenarios and the associated T_R bounds for $m_{\tilde{G}} \gtrsim 1$ GeV and for temperatures as low as 10^7 GeV. Taking into account the restrictive constraint from bound-state effects of long-lived negatively charged staus on the primordial ${}^6\text{Li}$ abundance [22], we find that $T_R \lesssim 10^7$ GeV is the highest cosmologically viable temperature of the radiation-dominated epoch in case of a standard thermal history of the Universe. This imposes a serious constraint on model building for inflation. Moreover, thermal leptogenesis seems to be strongly disfavored in the considered regions of the CMSSM parameter space.

With late-time entropy release, the obtained limit $T_R \lesssim 10^7$ GeV can be relaxed. For example, the dilution of the thermally produced gravitino yield by a factor of 10 relaxes the T_R bound by about one order of magnitude in regions where $\Omega_{\tilde{G}}^{\text{TP}}$ dominates $\Omega_{\tilde{G}}$. In the case of entropy production after NLSP decoupling, the yield of the NLSP prior to its decay, Y_{NLSP} , is reduced so that the BBN constraints can be weakened. Although the ${}^6\text{Li}$ bound is persistent, we find that it disappears provided Y_{NLSP} is diluted by a factor of $\Delta \gtrsim 10^4$.

We have discussed the viability of thermal leptogenesis in a cosmological scenario with entropy production after NLSP decoupling. We find that successful thermal leptogenesis can be revived in generic regions of the CMSSM parameters space for $M_{R1} \sim T_R \simeq 10^{13}$ GeV and $\Delta \gtrsim 10^4$, where M_{R1} is the mass of the lightest among the heavy right-handed Majorana neutrinos.

Remarkably, for a dilution factor of $\Delta \gtrsim 10^4$, the $\tilde{\tau}_1$ NLSP region with $m_{\tilde{\tau}_1} \lesssim 200$ GeV reopens as a cosmologically allowed region in the CMSSM with the gravitino LSP. A long-lived $\tilde{\tau}_1$ in this mass range could provide striking signatures of gravitino dark matter at future colliders [63, 64, 65, 66].

We are grateful to S. Blanchet, F. Hahn-Woernle, M. Plümacher, M. Pospelov, G. Raffelt, and Y.Y.Y. Wong for valuable discussions.

* Electronic address: jpradler@mppmu.mpg.de

† Electronic address: steffen@mppmu.mpg.de

- [1] A. D. Linde, *Particle Physics and Inflationary Cosmology*, (Harwood, Chur, Switzerland, 1990).
- [2] E. W. Kolb and M. S. Turner, *The Early Universe* (Addison-Wesley, Redwood City, 1990).
- [3] A. D. Linde, Phys. Lett. B **259** (1991) 38.
- [4] J. Wess and J. Bagger, *Supersymmetry and supergravity* (Princeton University Press, Princeton, 1992).
- [5] See S. P. Martin, hep-ph/9709356 and references therein.
- [6] M. Y. Khlopov and A. D. Linde, Phys. Lett. B **138** (1984) 265.
- [7] J. R. Ellis, J. E. Kim and D. V. Nanopoulos, Phys. Lett. B **145**, 181 (1984).
- [8] T. Moroi, H. Murayama and M. Yamaguchi, Phys. Lett. B **303**, 289 (1993).
- [9] M. Bolz, W. Buchmüller and M. Plümacher, Phys. Lett. B **443**, 209 (1998).
- [10] M. Bolz, A. Brandenburg and W. Buchmüller, Nucl. Phys. B **606**, 518 (2001).
- [11] J. Pradler and F. D. Steffen, Phys. Rev. D **75**, 023509 (2007).
- [12] T. Asaka, K. Hamaguchi and K. Suzuki, Phys. Lett. B **490** (2000) 136.
- [13] L. Roszkowski, R. Ruiz de Austri and K. Y. Choi, JHEP **0508** (2005) 080.
- [14] D. G. Cerdeno, K. Y. Choi, K. Jedamzik, L. Roszkowski and R. Ruiz de Austri, JCAP **0606**, 005 (2006).
- [15] F. D. Steffen, JCAP **0609**, 001 (2006).
- [16] M. Fukugita and T. Yanagida, Phys. Lett. B **174**, 45 (1986).
- [17] See W. Buchmüller, P. Di Bari and M. Plümacher, Annals Phys. **315**, 305 (2005) and references therein. For recent studies of flavor effects, see also S. Blanchet and P. Di Bari, hep-ph/0607330; S. Antusch and A. M. Teixeira, hep-ph/0611232.
- [18] J. Pradler and F. D. Steffen, in preparation.
- [19] C. Boehm, A. Djouadi and M. Drees, Phys. Rev. D **62** (2000) 035012.
- [20] J. R. Ellis, K. A. Olive and Y. Santoso, Astropart. Phys. **18** (2003) 395.
- [21] J. L. Feng, S. Su and F. Takayama, Phys. Rev. D **70**, 075019 (2004).
- [22] M. Pospelov, hep-ph/0605215.
- [23] K. Kohri and F. Takayama, hep-ph/0605243.
- [24] M. Kaplinghat and A. Rajaraman, astro-ph/0606209.
- [25] R. H. Cyburt, J. Ellis, B. D. Fields, K. A. Olive and V. C. Spanos, JCAP **0611** (2006) 014.
- [26] F. D. Steffen, hep-ph/0611027.
- [27] W. Buchmüller, K. Hamaguchi, M. Ibe and T. T. Yanagida, hep-ph/0605164.
- [28] M. Kawasaki, F. Takahashi and T. T. Yanagida, Phys. Lett. B **638** (2006) 8.
- [29] M. Kawasaki, F. Takahashi and T. T. Yanagida, Phys. Rev. D **74** (2006) 043519.
- [30] E. Braaten and T. C. Yuan, Phys. Rev. Lett. **66**, 2183 (1991).
- [31] E. Braaten and R. D. Pisarski, Nucl. Phys. B **337**, 569 (1990).
- [32] A. Brandenburg and F. D. Steffen, JCAP **0408**, 008 (2004); hep-ph/0406021; hep-ph/0407324.
- [33] M. Kawasaki, K. Kohri and T. Moroi, Phys. Lett. B **625** (2005) 7.
- [34] M. Kawasaki, K. Kohri and T. Moroi, Phys. Rev. D **71** (2005) 083502.
- [35] K. Kohri, T. Moroi and A. Yotsuyanagi, Phys. Rev. D **73**, 123511 (2006).
- [36] D. N. Spergel *et al.*, astro-ph/0603449.
- [37] W.-M. Yao *et al.*, J. Phys. G **33**, 1 (2006).
- [38] J. Hamann, S. Hannestad, M. S. Sloth and Y. Y. Y. Wong, astro-ph/0611582.
- [39] G. Anderson *et al.*, *In the Proceedings of 1996 DPF/DPB Summer Study on New Directions for High-Energy Physics (Snowmass 96), Snowmass, Colorado, 25 Jun -*

- 12 Jul 1996, *pp SUP107* [hep-ph/9609457].
- [40] A. Djouadi, M. Drees and J. L. Kneur, JHEP **0603** (2006) 033.
 - [41] J. R. Ellis, K. A. Olive, Y. Santoso and V. C. Spanos, Phys. Lett. B **588** (2004) 7.
 - [42] S. Borgani, A. Masiero and M. Yamaguchi, Phys. Lett. B **386** (1996) 189.
 - [43] A. Djouadi, J. L. Kneur and G. Moultaka, hep-ph/0211331. We use the version 2.34.
 - [44] G. Belanger, F. Boudjema, A. Pukhov and A. Semenov, Comput. Phys. Commun. **149**, 103 (2002); *ibid.* **174**, 577 (2006). We use the version 1.3.6.
 - [45] R. H. Cyburt, J. R. Ellis, B. D. Fields and K. A. Olive, Phys. Rev. D **67** (2003) 103521.
 - [46] R. Lamon and R. Dürer, Phys. Rev. D **73**, 023507 (2006).
 - [47] G. Sigl, K. Jedamzik, D. N. Schramm, and V. S. Berezinsky, Phys. Rev. D **52** (1995) 6682.
 - [48] K. Jedamzik, Phys. Rev. Lett. **84** (2000) 3248.
 - [49] K. Jedamzik, Phys. Rev. D **70** (2004) 063524.
 - [50] K. Jedamzik, Phys. Rev. D **74** (2006) 103509.
 - [51] R. J. Scherrer and M. S. Turner, Phys. Rev. D **31** (1985) 681.
 - [52] E. A. Baltz and H. Murayama, JHEP **0305** (2003) 067.
 - [53] M. Fujii and T. Yanagida, Phys. Lett. B **549** (2002) 273; M. Fujii, M. Ibe and T. Yanagida, Phys. Rev. D **69** (2004) 015006.
 - [54] K. Jedamzik, M. Lemoine and G. Moultaka, Phys. Rev. D **73** (2006) 043514; Phys. Lett. B **645** (2007) 222.
 - [55] M. Kawasaki, K. Kohri and N. Sugiyama, Phys. Rev. Lett. **82** (1999) 4168.
 - [56] M. Kawasaki, K. Kohri and N. Sugiyama, Phys. Rev. D **62** (2000) 023506.
 - [57] S. Hannestad, Phys. Rev. D **70** (2004) 043506.
 - [58] K. Ichikawa, M. Kawasaki and F. Takahashi, Phys. Rev. D **72** (2005) 043522.
 - [59] P. Gondolo and G. Gelmini, Nucl. Phys. B **360** (1991) 145.
 - [60] K. Kohri, M. Yamaguchi and J. Yokoyama, Phys. Rev. D **70** (2004) 043522.
 - [61] W. Buchmüller, P. Di Bari and M. Plümacher, Nucl. Phys. B **643** (2002) 367.
 - [62] W. Buchmüller, P. Di Bari and M. Plümacher, Phys. Lett. B **547** (2002) 128.
 - [63] W. Buchmüller, K. Hamaguchi, M. Ratz, and T. Yanagida, Phys. Lett. B **588**, 90 (2004).
 - [64] A. Brandenburg, L. Covi, K. Hamaguchi, L. Roszkowski, and F. D. Steffen, Phys. Lett. B **617**, 99 (2005); F. D. Steffen, hep-ph/0507003.
 - [65] H. U. Martyn, hep-ph/0605257.
 - [66] K. Hamaguchi, M. M. Nojiri and A. de Roeck, hep-ph/0612060.